Published in final edited form as:
Brain Res. 2010 March 8; 1318: 110–121. doi:10.1016/j.brainres.2009.12.075.

Altered Local Coherence in the Default Mode Network due to Sevoflurane Anesthesia

Gopikrishna Deshpande[1], **Chantal Kerssens**[2], **Peter Simon Sebel**[2], and **Xiaoping Hu**[1]

[1]Department of Biomedical Engineering, Georgia Institute of Technology and Emory University, Atlanta, GA, USA

[2]Department of Anesthesiology, Emory University School of Medicine, Atlanta, GA, USA

Abstract

Recently we introduced a robust measure, integrated local correlation (ILC), of local connectivity in the brain using fMRI data which reflects the temporal correlation of brain activity in every voxel neighborhood. The current work studies ILC in fMRI data obtained in the absence and presence of sevoflurane anesthesia (0%, 2%, and 1% end-tidal concentration, respectively) administered to healthy volunteers. ILC was determined specifically in regions of the default mode network (DMN) to address local changes in each state. In addition, a potential confound in analyses based on correlations due to signal-to-noise variations was addressed by wavelet denoising. This accommodated decreases in signal power commonly seen during anesthesia without artificially reducing derived correlations. Results showed that ILC was significantly reduced in the entire DMN during 2% sevoflurane yet recovered in the posterior and anterior cingulate cortices as well as inferior parietal cortex during 1% sevoflurane. By contrast, ILC remained attenuated prefrontally in the 1% condition, which indicates uncoupling of the frontal areas of DMN during light anesthesia. These results confirm widespread anesthetic-induced cortical suppression but also demonstrate that the local connectivity of the prefrontal cortex is rapidly reduced by sevoflurane. It remains to be seen whether these alterations arise locally as a direct consequence of anesthetic action on local neurons or are driven by distant changes in oscillations and activity elsewhere in the brain.

Keywords

low frequency fMRI fluctuations; resting state BOLD signal; local connectivity; default mode network; sevoflurane; volatile anesthesia; consciousness

1. INTRODUCTION

The loss and recovery of consciousness and their corresponding neural substrates is a central conundrum in anesthesiology and neuroscience. Rather than focusing on an isolated anatomical structure or neuronal process, network models (Crick *et al*., 2003; Mashour, 2004) take multiple, distributed regions of the brain into consideration and have attributed loss of

Corresponding Author: Xiaoping Hu, Ph.D. Wallace H. Coulter Department of Biomedical Engineering Georgia Institute of Technology and Emory University 101 Woodruff Circle, Suite 2001 Atlanta, GA 30322, USA Phone- 404 712 2615 Fax- 404 712 2707 xhu@bme.gatech.edu.

consciousness as induced by anesthesia to cognitive unbinding that result from reduced connectivity of functional networks in the brain. In support of this view, functional neuroimaging studies have demonstrated disrupted connectivity in thalamo-cortical networks (Ries *et al*., 1999; White *et al*., 2003), inter-hemispheric cortico-cortical networks (Peltier *et al*., 2005) and the default mode network (Peltier *et al*., 2006; Greicius *et al*., 2008) in the presence of anesthetic drugs. Another emerging view is that a complex of posterior brain areas is a common target for anesthetic-induced unconsciousness, and affects the brain's ability to integrate information, especially the flow of information between the front and back of the brain (Alkire, Hudetz & Tononi, 2008). In light of these hypotheses, inspection of local connectivity in the brain will further specify how different regions function and consequently, may contribute to normal brain activity and behavior. In this paper we investigate a measure of local connectivity in the brain by computing the temporal correlation of functional magnetic resonance imaging (fMRI) signals within a finite neighborhood of each voxel in the brain at different concentrations of an inhaled anesthetic.

fMRI-based local connectivity is conceptualized as carrying information about the coordination among neighboring sub-regions of the brain and will depend on the local anatomic structure and homogeneity of neuronal processes. Although fMRI correlates significantly with local field potentials and as such reflects key components of neural activity (i.e., the synaptic input and intracortical processing of a given area, Logothetis *et al*., 2001), temporal correlations in the fMRI signal may not necessarily be based on underlying anatomic connectivity (Honey *et al*., 2009). Therefore, measures such as ILC, as implemented in the current study, reflect local neural “synchrony” analogous to focal fMRI activations reflecting local neural “activity”. However, changes in local connectivity can be driven by altered neuronal dynamics in a distant region. Therefore, ILC is a valuable measure for assessing regional functional homogeneity rather than localized anesthetic action. As such, it yields a new perspective on anesthetic action that emphasizes network effects on a local scale.

The concept of fMRI-based local connectivity has gained significance in neuroimaging literature with studies (Deshpande *et al*., 2009; Liu *et al*., 2006; Zang *et al*., 2004) demonstrating how information on local connectivity complements information on distributed, long-range connectivity. The latter captures synchronous activity between remote regions of interest (ROIs) rather than neighboring sub-regions within an ROI. For example, increased local connectivity in Alzheimer's patients is thought to compensate for decreased distributed connectivity observed in these patients (Liu *et al*., 2008). Local connectivity functionally parcellates the brain, and the parcellation is distinctly different in individuals with schizophrenia as compared to healthy controls (Shi *et al*., 2007). In addition, local connectivity changes can be a marker of various neurophysiological disorders such as attention deficit/hyperactivity disorder (Zhu *et al*., 2008), clinical depression (Yuan *et al*., 2008; Yao *et al*., 2009) and Parkinson's disease (Wu *et al*., 2009), as well as normal cognitive development in healthy children (Pang *et al*., 2009). Among the various approaches to measure local connectivity, we recently introduced a robust measure, integrated local correlation (ILC), to measure local connectivity in the brain from fMRI data (Deshpande *et al*., 2009). In the present study, ILC was applied to resting state fMRI data from human subjects inhaling 1% and 2% sevoflurane, a commonly used volatile anesthetic.

The effects of sevoflurane on brain function have been studied with fMRI in sensory, motor and higher association areas (Kerssens *et al*., 2005; Ramani *et al*., 2007; Marcar *et al*., 2006; Heinke *et al*., 2001). While it is evident that sevoflurane dose-dependently attenuates task-related fMRI responses, effects on task-independent and spontaneous fMRI activity were so far examined only in the motor cortex (Peltier *et al*., 2005). These spontaneous, very low-frequency fluctuations (<0.1 Hz) are observed while subjects are not engaged in a particular task (hence, `resting-state') and have been shown to be correlated across brain regions that

serve the same function (hence, `functional connectivity', Biswal *et al*., 1995). Previous studies have shown that functional connectivity in the motor cortex is attenuated by sevoflurane (Peltier *et al*., 2005). Given their functional specialization, motor regions and many other regions in the brain are typically more engaged during an active task as compared to resting state. In contrast to these task-networks, a specific set of regions has been found to be more active during rest instead. This `default mode network' (DMN) almost invariably includes the posterior and anterior cingulate cortices, dorsolateral and medial prefrontal cortex,and inferior parietal cortex (Raichle *et al*., 2001; Greicius *et al*., 2003). Though its precise role and function is yet unclear, the DMN appears to be involved in some form of self-awareness and introspection, which renders it relevant to studies of consciousness Reduced or absent DMN connectivity is seen in brain dead but not vegetative state patients (Boly *et al*., 2009),), during meditation (Pagnoni *et al*., 2006; 2008) and under pharmacologically induced sedation (Greicius *et al*., 2008), ostensibly subserving altered states of consciousness. Most recently, the network was shown to uncouple during deep sleep when reduced functional connectivity of the frontal cortex was observed (Horovitz *et al*., 2009). Even in fully awake subjects, the prefrontal region appears to interact preferentially with parietal attention networks whereas the posterior cingulate region interacts with prefrontal motor control circuits (Uddin *et al*., 2009) suggesting that the DMN may be less homogeneous that previously thought. Both regions seem to directly modulate activity in these respective networks rather than the other way around (Uddin *et al*., 2009). This may explain why DMN activity and resting states in general are relevant to task-related brain activity and normal behavioral function (Boly *et al*., 2007; Eichele *et al*., 2008; Wig *et al*., 2008). Also, these studies indicate that functional differentiation within the DMN is important and valuable to examine.

We have hypothesized that anesthesia alters DMN activity and provided preliminary evidence in support of this notion by demonstrating reduced distributed DMN connectivity during sevoflurane anesthesia (Peltier *et al.*, 2006). Functional differentiation *within* the DMN, however, can be readily examined with local connectivity measures such as ILC. By inspecting the functional integrity of individual regions as measured by ILC, changes within network components that go unnoticed in examinations of distributed connectivity (which captures the temporal correlation *between* regions), may be observed. Consequently, ILC could be a useful tool for testing brain differentiation hypotheses and information integration theories of anesthetic action.

A serious source of confound in any analysis of time series correlations is a reduction in signal power, which degrades the signal to noise ratio (SNR) and may artificially lower correlation values. Critically, the intrinsic state of the brain may not have changed yet conclusions to the contrary are drawn based on the correlation values. The vasodilatory effect of sevoflurance (Matta *et al.*, 1999; Kolbitsch *et al.*, 2001; Kaisti *et al.*, 2002; 2003) has the potential to decrease the BOLD signal power (Stefanovic *et al.*, 2006), a confound we addressed in our analysis by denoising the fMRI time series using wavelets, thereby preventing the degradation of SNR.

2. RESULTS AND DISCUSSION

2.1 Physiological Parameters

All subjects maintained normal physiologic parameters during anesthetic administration and no adverse events occurred at any time during or after the study. End-tidal carbon dioxide increased marginally between the 1% and 2% sevoflurane conditions (light vs. deep state, mean ± standard deviation: 38.2 ± 3.1 vs. 38.7 ± 4.6 mmHg, respectively) but not significantly (Wilcoxon Ranks Test, p=0.35). Respiratory rates in the light state (18 ± 2 breaths per minute, brpm), deep state (21 ± 3 brpm) and the awake state (no anesthesia, 24 ± 5 brpm) were not significantly different from each other (Friedman Test, p=0.07). We note that breathing was

regular at all times and no volunteer stopped breathing at any time nor were any volunteers excluded due to respiratory irregularities.

Heart rate showed a similar, dose-*independent* trend over time between the awake (55.9 ± 5.4 beats per minute, bpm), deep (53.4 ± 7.5 bpm), and light states (51.9 ± 6.6 bpm, Friedman Test, p=0.22). Mean arterial pressure decreased significantly as a function of dose (awake: 87.5 ± 12.1 mmHg; Light: 70.8 ± 3.4; Deep: 68.5 ± 4.5 mmHg, Friedman test, p<0.01). These data are consistent with the literature and suggest modest hemodynamic and respiratory changes in the presence of sevoflurane (Matta *et al.*, 1999; Lorenz *et al.*, 2001; Cho *et al.*, 1996).

2.2 Physiological Artifacts

The mean value of $C_{\text{mean}}(f)$, which is the mean spectral cross-coherence in the neighborhood of the voxel, obtained from all the subjects from each of the three states are shown in Fig. 1. Note that the frequency ranges from 0.01 Hz to 0.665 Hz, which is half the sampling frequency. Intuitively, the spectral cross-coherence in the neighborhood of the voxel provides a frequency-specific decomposition of the corresponding ILC. The following observations are pertinent. The high frequency coherence components (>0.1 Hz), which typically contain the effects of physiological artifacts, were significantly lesser in magnitude and remained relatively constant between the three states in comparison to the low frequency coherence components (<0.1 Hz) which are thought to be physiologically relevant (Razavi *et al*., 2008). Therefore, it can be inferred that the ILC differences between the three states were mainly driven by the differences in the low frequency coherence components. A comparison of the mean spectra obtained from the fMRI time series inside the brain and downsampled physiological data revealed that in comparison to the power in the fMRI time series, the latter's power was negligible (Fig. 2). This verified that downsampling did not alias the physiological rhythms into the low frequency band, which is to be expected since the TR (750 ms) was relatively small. Therefore, neither the physiological measurements themselves nor their purported effect on local correlation suggested that the dependence of ILC on anesthesia could be attributed to physiological confounds.

2.3 Local Connectivity during Anesthesia

The group ILC maps in the awake, deep and light states, which were studied in that order, are shown in Fig. 3. It can be seen that there was a general reduction in local connectivity between the awake and deep states., and the mean ILC of all grey matter regions in the brain (global mean ILC) significantly decreased between the two (p<0.05). In the light state that followed the deep state, the mean ILC significantly increased in comparison to the deep state (p<0.05). These results indicate dose-dependent changes in local connectivity in all grey matter regions of the brain.

Although 2% end-tidal sevoflurane reduced ILC globally including the DMN, notable differences between local connectivity in the DMN and other grey matter areas were apparent. First, the default mode regions had a significantly higher ILC compared to the global mean ILC across all subjects and states (p<0.05). This may be tied to the exceptionally high metabolic rate exhibited by these regions in resting state (Raichle *et al.*, 2001). Second, unlike the global mean ILC, the prefrontal regions of the DMN did not show a significant difference between ILC in the deep and light states. The overall observation is that normalization of local connectivity in the light state was substantial in posterior cingulate cortex, anterior cingulate cortex and inferior parietal cortex but negligible in the medial and lateral prefrontal regions. Default-mode-specific ILC values for individual subjects are shown in Fig. 4. Based on these observations, it is evident that the changes in local coherence in the DMN did not simply reflect those seen globally in the presence of sevoflurane anesthesia. Instead, local coherence remained remarkably high in some regions of the DMN, but was markedly disrupted in prefrontal regions.

We focused on the DMN given the network's relevance to altered states of mind and consciousness. Previous work has shown reduced connectivity between the regions of the DMN with increasing concentrations of sevoflurane (Peltier *et al.*, 2006) and in the presence of midazolam, an intravenous sedative agent (Greicius *et al*., 2008). We demonstrate here that local connectivity within individual regions of the DMN is also reduced by sevoflurane anesthesia. However, local connectivity did not change uniformly across anesthesia concentrations, but was lost in prefrontal regions of the DMN at concentrations of sevoflurane that left the local connectivity in posterior regions intact. Effectively, a disconnect between the front and back of the brain, which may be interpreted as uncoupling of the frontal areas of DMN, was found at 1% sevoflurane. At higher concentrations (2% sevoflurane), all studied DMN regions exhibited reduced local connectivity.

At the concentrations studied here, sevoflurane is known to reduce cerebral blood flow and oxygen metabolism especially (i.e., beyond any global reductions) in the midbrain (thalamus), posterior lateral and medial cortex (cuneus, precuneus, inferior parietal lobule) and cerebellum (Kaisti *et al*, 2002; 2003). Therefore, the loss of local connectivity we observed prefrontally may not necessarily suggest that the anesthetic acted locally in the prefrontal regions per se but rather may suggest a change in neural dynamics that is at least in part driven by a region elsewhere in the brain on which the anesthetic acts directly.. Irrespective of whether the anesthetic acts directly on the prefrontal regions or not, our results do suggest that the prefrontal cortex is sensitive to anesthesia and shows reductions in local connectivity at relatively low anesthetic concentrations. This sensitivity may explain why front-to-back interactions, as measured by transfer entropy in rats, decrease markedly during anesthesia while feed-forward interactions from the back of the brain remain intact (Imas *et al.*, 2005). Resting-state fMRI data sets do not provide insight into the temporal order of events within a single experimental scan, but an outline of local and global cascades can be tentatively inferred from the differential response of brain regions to anesthesia exposure obtained in this study.

The dissociation between regions of the DMN during inhalation of 1% end-tidal sevoflurane clearly confirms that general anesthesia is not a uniform entity (Veselis *et al.*, 2001; Franks, 2006) but affects regions differentially and perhaps on more than one level (i.e., local effects on neuronal activity vs. distributed effects on brain connectivity). To the extent that the DMN supports elements of consciousness, our study strongly supports network theories of consciousness that emphasize the integrity of the frontal and parietal cortex, as well as the interactions between them (Alkire, Hudetz & Tononi, 2008). Although we did not examine such interactions directly, a fronto-parietal disconnect is implied in our results. These results tie in with anterior-posterior dissociations that have been reported to occur upon loss of consciousness as measured by scalp EEG in humans (John *et al.*, 2001) and event-related potential studies in rats (Imas *et al*., 2005). In contrast to these existing studies, however, the present findings are based on a hemodynamic measure (fMRI) rather than electrophysiology and derive from very low frequency oscillations (<0.1 Hz) as opposed to fast (30 – 80 Hz). Nevertheless, a similar phenomenon - front-to-back disconnect – was observed. This suggests that resting-state fMRI has merit in investigations of cognitive function and impairment, especially because it is readily applied in humans, is noninvasive and task-independent. Furthermore, the inspection of local connectivity using ILC seems to add specificity to measures of distributed connectivity, in this study by implicating the prefrontal cortex rather than other brain regions in connectivity changes at low anesthesia concentrations.

While these physiological changes presumably underlie some of the behavioral impairments associated with sevoflurane anesthesia (Galinkin *et al.*, 1997, Ibrahim *et al.*, 2001), such associations were not addressed in the current study because probing function, by definition, is incompatible with assessment of the resting state. We, therefore, cannot comment on the functional status of subjects at the time of study. However, we speculate that consciousness

was virtually absent under 2% end-tidal sevoflurane and was disrupted during 1% sevoflurane. This sits well with the clinical concept of MAC, the minimum alveolar concentration required to prevent response to a painful stimulus (surgical incision) in half the population, which is roughly 2% sevoflurane in this age group (Nickalls & Mapleson, 2003). Future studies are recommended to include a low-level (passive) task that allows collection of response data such as reaction times or accuracy, or to collect more complex task data in a run in close succession of the resting-state acquisition.

2.4 Caveats

The limitation of the current study is that the link between our measurement and neuronal function is only as tenuous as that between fMRI and neuronal function. According to Logothetis *et al* (2001), fMRI can be construed as a convolution of the local field potentials (LFP) with the hemodynamic response function and subsequent downsampling due to the slow speed of MR acquisition. Since both convolution and downsampling are linear operators, instantaneous covariance between LFPs from neighboring neuronal units will still be preserved in the fMRI time series obtained from the neighboring voxels corresponding to those neuronal units (See Wei, 1982 for a theoretical proof), albeit with a different magnitude. The neuronal units under consideration are “neighboring” only with respect to the spatial resolution of fMRI and may not be adjacent on a neuronal scale. However, it may still correspond to a functionally homogeneous region. Since LFPs are indicative of the pre-synaptic input activity of a neuronal population, covariance between neighboring LFPs and hence between neighboring fMRI voxel time series may be indirectly linked to synchronous pre-synaptic neuronal activity. It is to be noted here that since the covariance in LFPs is translated into covariance in fMRI, the link between our measurement and neuronal function is only as good as the link between fMRI and neuronal function.

Notwithstanding the discussion so far, the results presented here should be only cautiously generalized, if at all. The effect of anesthetic agents and their mechanism of action on brain cells and systems are not properly understood yet known to diverge (Franks, 2006). Indeed, it should be recognized that recent studies have reported *increased* temporal synchrony in the fMRI BOLD signal depending on the region of interest using intravenous drugs such as midazolam (Kiviniemi *et al.*, 2005; Greicius *et al.*, 2008) and propofol (Kerssens *et al.*, 2008). Moreover, entities such as consciousness may not be a monolith and its neural substrates could vary depending on whether changes are induced artificially (sedatives) or naturally (sleep) (Mashour, 2004). In light of these notions, our results should be interpreted within the specifics of our experiment.

2.5 Summary

We report gradual changes in local connectivity in the human brain at 1 and 2% end-tidal sevoflurane. ILC, a robust measure of local connectivity derived from fMRI data, was examined in core regions of the default mode network (DMN). Data were denoised using wavelets in order to remove the dependence of ILC on changes in signal power and hence, SNR. The results suggest that local connectivity was reduced globally and in the DMN during 2% end-tidal sevoflurane. During 1% end-tidal sevoflurane, however, local connectivity recovered in posterior cingulate, anterior cingulate, and inferior parietal cortices but not the prefrontal cortex. These results suggest uncoupling of the frontal areas of DMN at low levels of anesthesia and a sensitivity of the prefrontal cortex to anesthetic action. Further studies are required to ascertain whether this is a result of local anesthetic action on the frontal areas or are driven by local action by the drug elsewhere in the brain. This work demonstrates the utility of ILC for noninvasive characterization of local brain function within and across different brain states.

3. EXPERIMENTAL PROCEDURES

3.1 Participants

Six right-handed male volunteers (22 – 24 years old) took part in this study which was approved by the institutional review board of Emory University. As part of the consent process participants were informed of the overall anesthetic procedure, the different concentrations that would be used, and associated effects on sleepiness. They were specifically informed of "invasive" procedures such as placement of a laryngeal mask airway (breathing device) and intravenous needle, and known risks associated with such procedures and anesthesia. In order to reduce the probability of adverse events and in adherence to good anesthetic practice, subjects were required to fast for 8 hours prior to study and they were carefully screened prior to inclusion as to assure their health and to minimize risk. Screening consisted of a physical exam and medical history (performed by PS) which identified risk factors for receiving anesthesia. Additionally, a self-report questionnaire assessed risk factors for MRI scanning. If there were doubts about the appropriateness of subject participation in relation to a number of predetermined exclusion criteria, subjects were not included in the study.

3.2 Anesthesia

The study was designed to assess the graded effect of sevoflurane on brain function using three states: awake, deep and light, in that order. This order was preferred over one progressing from light to deep in order to critically test dose-dependency of anesthesia effect on brain activity: If dose-dependent, brain function should recover (partially) in the light state following a deep state. If not, carry-over effects from the deep state may be implicated and/or the dose-response relationship may be nonlinear. By having the light state follow the deep state, both issues could be explored. States were achieved by administering 0%, 2% and 1% end-tidal sevoflurane, respectively. At each level, resting state and task-related BOLD fMRI data were acquired, in that order, the latter of which were reported elsewhere (Kerssens *et al.*, 2005). For present purposes, the awake state corresponded to a normal resting-state scan without anesthesia.

An anesthesiologist (PS) was responsible for the anesthetic procedure and continuously present in the scanner room during sevoflurane administration together with an anesthetist. Prior to the induction of anesthesia, volunteers gargled with 4% viscous lidocaine in order to facilitate subsequent placement of a breathing tube (laryngeal mask airway). Anesthesia was then induced with sevoflurane in oxygen using the single-breath technique. After securing a laryngeal mask airway, sevoflurane concentration was held constant at 2% for 15 minutes in order to allow pseudo-equilibration with brain and achieve a steady-state deep anesthetic. At this point, resting state scans corresponding to the deep state were obtained. Subsequently, the end-tidal sevoflurane concentration was adjusted to 1% and held constant for 15 min prior to scanning in order to achieve the light anesthetic state and corresponding resting state scans. Volunteers breathed spontaneously throughout the anesthetic procedure and oxygen flow was not adjusted after induction. Standard anesthetic monitoring was employed throughout the experiment, including end-tidal carbon dioxide monitoring via a sample line attached to the anesthetic circuit. The monitoring was in accordance with the American Society of Anesthesiologists practice standard parameters and included inspired and expired respiratory gases (including sevoflurane), pulse oximetry (blood oxygen saturation), blood pressure, heart rate, and respiratory rate. The physiological data were continuously collected and monitored yet manually recorded at regular intervals for data reporting purposes. After the anesthesia procedure, subjects were taken to the post-anesthesia care unit until they met Aldrete score 10 (oriented, awake, stable/normal physiology). They had something to eat and drink and were tested for recognition memory once the subject and anesthesiologist felt anesthesia recovery was complete. Subjects were told not to drive for the remainder of the day and had arranged for appropriate means of transportation or an escort home. We followed up on their physical

and mental well being per telephone call the next day. All subjects indicated to feel fine upon follow-up.

3.3 Data Acquisition

Resting-state echo planar imaging (EPI) data were acquired on a 3T Siemens Trio, with pulse sequence parameters: TR= 750 ms; TE= 35 ms; FA= 20°; FOV= 22 cm; 10 axial slices with 5 mm slice thickness, 280 volumes per slice and an in-plane resolution of 3.44 mm × 3.44 mm. In addition, T_1-weighted anatomical images with 1 mm isotropic resolution were acquired using a magnetization prepared rapid gradient echo (MPRAGE) sequence with TR/TE = 2600/3.93 ms and FA=8°.

3.4 Data Analysis

3.4.1 Pre-processing—The motion parameters for all the subjects were reviewed using Brainvoyager™ 2000 (Ver 4.9 © Rainer Goebel and Max Planck Society, Maastricht, The Netherlands. www.brainvoyager.com). One subject was excluded from the analysis due to severe gross head motion at the beginning of scanning under anesthesia. In the remaining subjects motion was not significant and was corrected using the Brainvoyager™ 2000 software. Subsequently, slice scan time correction and linear detrending (<0.008 Hz) were performed to remove very low frequency scanner drifts. The regions corresponding to the default mode network were identified in the resting-awake state using independent component analysis (ICA) (Greicius *et al.*, 2004) and a mask formed from the anatomic data. The resting-state default mode mask was transformed into the MNI (Montreal Neurological Institute) space (Evans *et al.*, 1993) and is shown in Fig. 5. The default mode masks for analyzing the deep and light states were generated by transforming the MNI space mask to their respective native EPI space. The transformations between EPI and MNI space were carried out using SPM2 (Wellcome Department of Cognitive Neurology, London, UK; http://www.fil.ion.ucl.ac.uk).

3.4.2 Wavelet Denoising—Wavelet denoising is a procedure where in the time series is decomposed into “approximate” and “detail” wavelet coefficients by using a filter bank comprising complementary low pass and high pass filters, respectively. In the wavelet transform domain, the signal energy gets packed into a few coefficients, enabling the separation of the signal from noise. Soft thresholding the noise coefficients (Donoho, 1995) and inverse wavelet transforming (Strang *et al.*, 1996) the remaining coefficients will render the signal in the time domain without the noise. It is to be noted that, unlike global signal regression, wavelet denoising only separates the signal from the noise using the representation of the time domain signal in a vector space spanned by the wavelet basis functions and hence does not alter the properties of the signal of interest and does not reuse any part of the data, as a consequence of which, it does not introduce anti-correlations in the data. We performed simulations to show that wavelet denoising is effective in minimizing the contribution of noise in the correlation coefficient between time series and hence ILC (see the appendix for details). Further, we demonstrated using real fMRI data that the autocorrelation function (ACF) of the difference time series (original-denoised time series) inside the brain significantly correlated with the ACF of the time series outside the brain (Pearson's correlation coefficient 0.87, $p<0.01$), proving the applicability of denoising for fMRI (Appendix). Subsequent to pre-processing, every voxel time series within the brain mask was denoised using sixth order Daubechies wavelets with five levels of wavelet decomposition and soft thresholding. The choices of these parameters were not critical to denoising performance and most of the choices using soft thresholding (Donoho, 1995) showed that the ACF of the difference time series inside the brain significantly correlated with the ACF of the time series outside the brain. The denoised data was used to calculate ILC as described below.

3.4.3 Integrated Local Correlation—ILC of a voxel is defined as the integral of the spatial correlation function at that location as given below (Deshpande *et al.*, 2009). The spatial correlation function represents the temporal correlation of the voxel under consideration with its neighbors.

$$ILC\left(\vec{s}\right) \cong \sum_{x}\sum_{y} \frac{\sum_{n=0}^{N-1}\left[a_{\vec{s}}(n).b_{xy}(n)\right]}{\sqrt{\sum_{n=0}^{N-1}\left[a_{\vec{s}}(n)\right]^2.\sum_{n=0}^{N-1}\left[b_{xy}(n)\right]^2}} \quad (1)$$

where $\vec{s}$ is the position of the voxel under consideration and $a_{\vec{s}}(n)$ is the time course for that voxel. The neighboring voxels are represented by $b_{xy}(n)$ where x and y are indices relative to the voxel under consideration.

As in Deshpande *et al.* (2009), we employed a neighborhood size of 60 × 60 mm^2 in this work. ILC calculations were performed using custom software written in MATLAB (The MathWorks Inc, Massachusetts). ILC maps were generated by calculating ILC values corresponding to each voxel within the brain using the denoised data. This procedure was carried out in the native EPI space of the data. The ROI specific ILC values for the default mode network regions – posterior cingulate cortex (PCC), anterior cingulate cortex (ACC), bilateral inferior parietal cortex (IPC) and frontal cortex (FC) – were derived by applying the default mode masks to the ILC maps and calculating the mean ILC values within each ROI. Within the default mode mask, the four ROIs were identified based on their anatomical location. Although these ROIs are not inclusive of all the regions in the default mode network, they were consistently identifiable in the ICA components of all the subjects and include the main regions identified and studied by others (Raichle *et al*., 2001; Greicius *et al*., 2003, 2004; 2008). The frontal ROI consisted of medial and lateral prefrontal regions. The statistical significance of the change in ILC values from awake to deep state and that from deep to light state was ascertained by performing a Wilcoxon rank sum test (Wilcoxon, 1945) between the voxel ILC values of each ROI in different states. The non-parametric Wilcoxon rank sum test was employed instead of the t-test since ILC distributions have been shown to be not normal (Deshpande *et al.*, 2009).

3.4.4 Physiological Artifacts—In order to determine whether the ILC obtained from denoised data had any contribution from physiological confounds such as respiratory and cardiac pulsations, the local correlation in the neighborhood of each voxel was spectrally decomposed using spectral cross-coherence. Accordingly, for each voxel time series $a_{\vec{s}}(n)$ and its neighbor $b_{xy}(n)$, their auto power spectral densities $P_a(f, s)$ and $P_b(f, x, y)$ as well as the their cross power spectral density $P_{ab}(f,s,x,y)$ were calculated using Welch's method (Hayes, 1996). The spectral cross-coherence between the time series, which spectrally decomposes the contribution of different frequency components to the time-domain cross-correlation between $a_{\vec{s}}(n)$ and its neighbor, $b_{xy}(n)$, was evaluated as follows.

$$C\left(f,\vec{s},x,y\right) = \frac{\left|p_{ab}\left(f,\vec{s},x,y\right)\right|^2}{P_a\left(f,\vec{s}\right)\times P_b(f,x,y)} \quad (2)$$

The mean spectral cross-coherence in the neighborhood of the voxel under consideration $a_{\vec{s}}(n)$ was calculated as given below.

$$C_{mean}\left(f,\vec{s}\right)=\frac{\sum_x\sum_y C\left(f,\vec{s},x,y\right)}{xy-1} \quad (3)$$

The mean and standard deviation of the quantity in Eq. 3 was evaluated over all the voxel positions inside the brain for which ILC was calculated, to obtain one cross-spectral coherence function $C_{mean}(f)$ for each of the three states – awake, deep and light. This quantifies the contribution of different frequency components to the global changes in ILC between the three states. First, we evaluated whether the high frequency coherence components (>0.1 Hz), which typically contains the effects of physiological artifacts, were significant in comparison to the low frequency coherence components (<0.1 Hz) which are thought to be physiologically relevant (Razavi *et al*., 2008). Second, we ascertained the band of frequency which drove the ILC changes between the three states. Third, we downsampled the cardiac and respiratory data to match the sampling rate of fMRI data in order to ascertain whether the high frequency components that they carry may have been aliased to the low frequency band.

Acknowledgments

The authors acknowledge the support by Georgia Research Alliance and NIH grant R01EB002009. Our special thanks to Dr. Scott Peltier at University of Michigan for helping out with physiological data.

APPENDIX

A.1 Simulations

When examining correlation between two signals, the power of the signals versus the noise variance needed to be considered. In the absence of noise, the correlation coefficient between two fMRI time series does not depend on the signal power. This is not the case in the presence of random noise, in which case the correlation of the two signals decreases with the SNR of the data, i.e. decreasing with the signal power if the noise variance remains the same. The effect of noise, hence the dependence on the signal power, can be lessened if the noise component of the time series is reduced. We addressed this issue by wavelet denoising. The effectiveness of denoising is first illustrated using simulations described below.

Let *x(t)* and *y(t)* be two heavy sine time series as shown below.

$$x(t)=A\left(4\times sin\left(4\times\pi\times t\right)-sign\left(t-0.3\right)-sign\left(0.72-t\right)\right) \quad (A1)$$

$$y(t)=A\left(4\times sin\left(4\times\pi\times t\right)+4\times cos\left(4\times\pi\times t\right)-sign\left(t-0.3\right)-sign\left(0.72-t\right)\right) \quad (A2)$$

Where *sin*, *cos* and *sign* are the sine, cosine and signum functions, respectively. The heavy sine functions have been previously used to illustrate the effectiveness of wavelet denoising (Donoho, 1993).

The amplitude scaling factor of both *x(t)* and *y(t)*, A, varied from 1 (no scaling) to 0.33 (amplitude decreased by three times). Gaussian distributed random noise of a standard deviation of one, generated using a random number generator, was added to *x(t)* and *y(t)* to produce *x′(t)* and *y′(t)*. The noise corrupted time series were denoised using wavelets resulting in time series *x″(t)* and *y″(t)*. For each scaling factor, the correlation coefficients *R′* and *R″*

between the noise corrupted and denoised time series, respectively, were obtained. The mean values of R' and R'' over 1000 realizations of the noise process were computed.

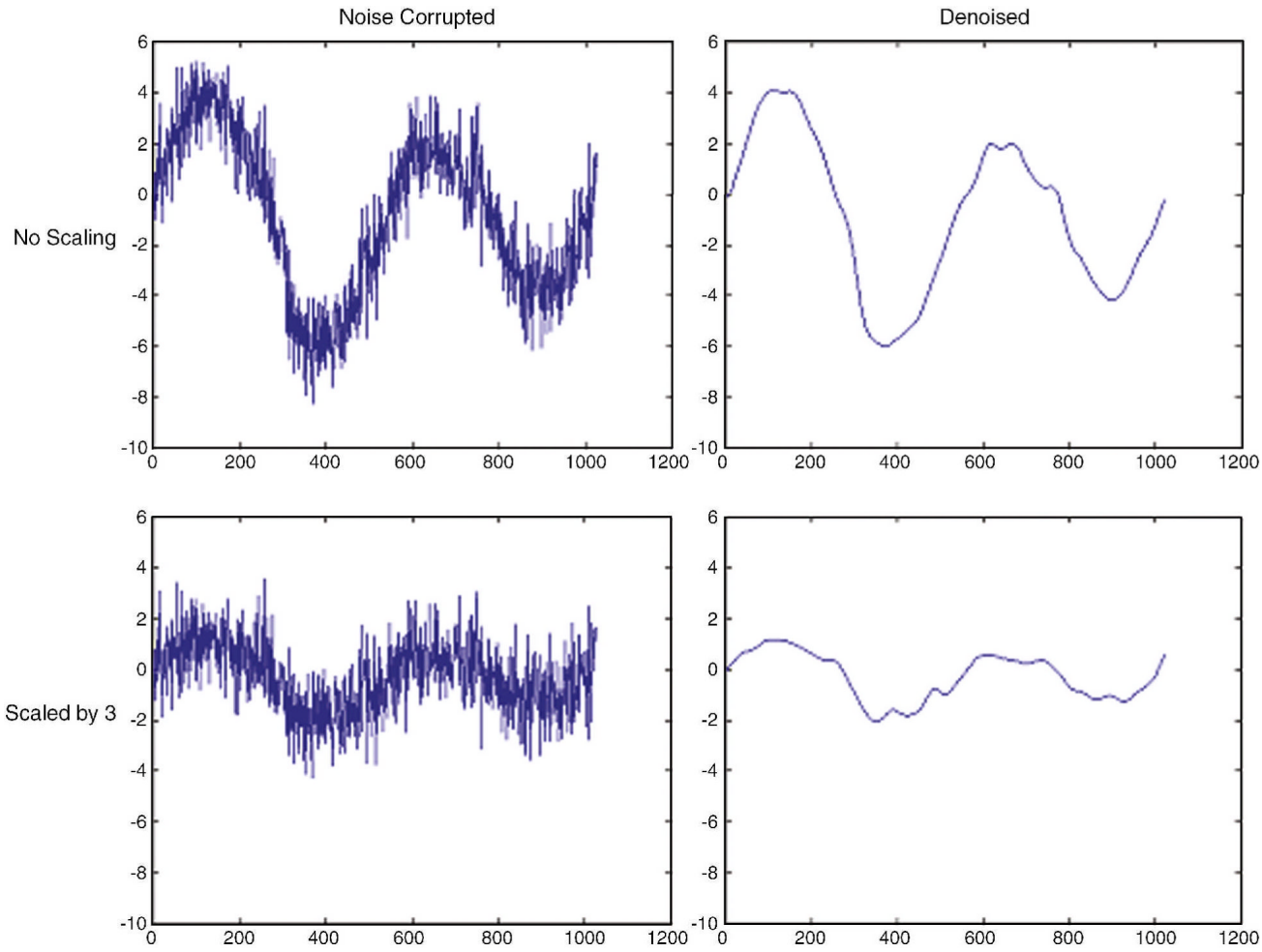

Figure A1.
Original (top) and scaled (bottom) time series x(t) with and without denoising (right and left panels, respectively). This illustrates the effectiveness of wavelet denoising for removing only the random fluctuations introduced by noise while retaining the signal of interest.

A.2 Simulation Results

Fig. A1 shows the original and scaled simulated time series with and without denoising. Fig. A2 illustrates the variation of mean R' and R'' as a function of the signal amplitude. R' decreased with the reduction of signal amplitude as predicted. However, R'' remained relatively constant illustrating that denoising has the potential to lessen the SNR dependence of the correlation coefficient. Also, the correlation coefficient between the original time series $x(t)$ and the denoised time series $x''(t)$ was 0.997. This shows that wavelet denoising effectively removed the noise introduced by the random number generator.

The denoising is valid to fMRI data if the difference time series between original and denoised time series contains only noise and not the signal of interest. We verified that this was the case by calculating the autocorrelation function (ACF) of the difference time series inside the brain and compared it to that of the noise time series outside the brain. ACF is depictive of the rate of the decrease in correlation with increasing temporal distance from a reference time point within the time series. Since the time series outside the brain mainly contains random noise

whose adjacent time points are not highly correlated, its ACF should decrease exponentially as a function of time. Fig. A3 compares the ACFs of the mean of all the difference time series inside the brain and the mean of all the time series outside the brain. It can be seen that both ACFs exponentially decreased suggesting that they arise from random noise. Furthermore, the two ACFs were very similar (Pearson's correlation coefficient 0.87, $p<0.01$) indicating that the difference time series inside the brain and the noise time series outside the brain, correspond to the random noise of similar nature. These results show that wavelet denoising removes mainly the noise and retains the signal of interest in the fMRI data. Therefore, post wavelet denoising, decreased correlation within a neighborhood in the brain during anesthesia can be attributed to lower synchrony between fMRI time series rather than degraded SNR resulting from lower signal power under anesthesia.

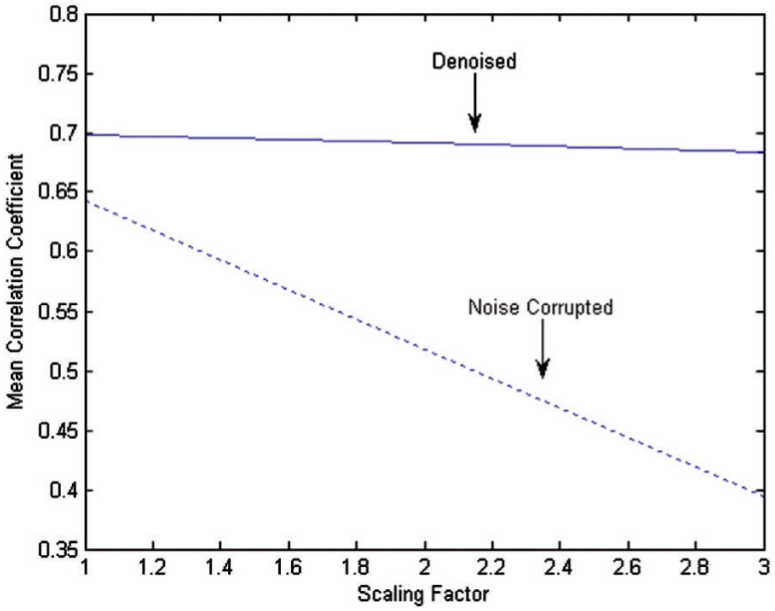

Figure A2.

The variation of mean R′ (dotted line) and R″ (solid line) as a function of the scaling factor. This illustrates that, in the presence of noise, a decrease in signal amplitude (i.e. increase in scaling factor) can lead to artificially reduced correlation even though the synchrony between the signals remain unaltered. With wavelet denoising, the dependence of correlation on signal amplitude is largely reduced as shown by the relatively flat line obtained from denoised data

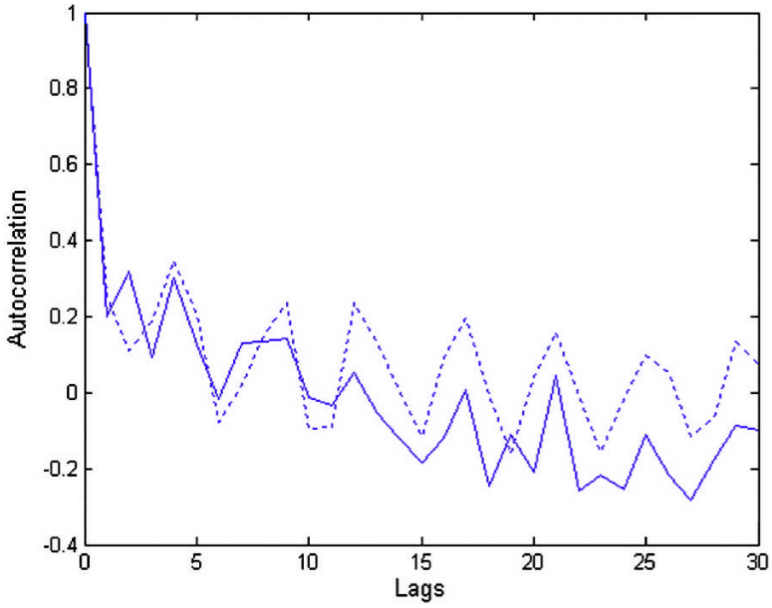

Figure A3.
The autocorrelation functions of the difference time series between the original and denoised signals inside the brain (solid line) and the mean time series outside the brain (dotted line) obtained from fMRI data acquired during the deep anesthetic state. The difference time series between the original and denoised signals inside the brain is a measure of the noise removed by wavelet denoising from brain tissue. The mean time series outside the brain represents the measurement noise introduced by the scanner. Since the autocorrelation function, which is a signature of noise characteristics, of both the time series were closely matched, it can be inferred that wavelet denoising removed only the measurement noise and not the signal of interest from the brain tissue.

Non-standard Abbreviations

(ILC)	Integrated local correlation
(DMN)	Default mode network
(ICA)	Independent component analysis
(ACF)	Autocorrelation function
(PCC)	Posterior cingulate cortex
(ACC)	Anterior cingulate cortex
(IPC)	Inferior parietal cortex
(FC)	Frontal cortex
(MAC)	Minimum alveolar concentration

REFERENCES

Alkire MT, Haier RJ, Barker SJ, Shah NK, Wu JC, Kao YJ. Cerebral metabolism during propofol anesthesia in humans studied with positron emission tomography. Anesthesiology 1995;82:393–403. [PubMed: 7856898]

Alkire MT, Gruver R, Miller J, McReynolds JR, Hahn EL, Cahill L. Neuroimaging analysis of an anesthetic gas that blocks human emotional memory. Proc Natl Acad Sci USA 2008a;105(5):1722–1727. [PubMed: 18227504]

Alkire MT, Gruver RL, Cahill L. Desflurane suppresses human working memory areas without changing amygdala-hippocampal connectivity. Anesthesiology 2008b;109:A835.

Alkire MT, Hudetz AG, Tononi G. Consciousness and anesthesia. Science 2008;322(5903):876–880. [PubMed: 18988836]

Biswal B, Yetkin FZ, Haughton VM, Hyde JS. Functional connectivity in the motor cortex of resting human brain using echo-planar MRI. Magnetic Resonance in Medicine 1995;34:537–541. [PubMed: 8524021]

Boly M, Balteau E, Schnakers C, Degueldre C, Moonen G, Luxen A, Phillips C, Peigneux P, Maquet P, Laureys S. Baseline brain activity fluctuations predict somatosensory perception in humans. Proc Natl Acad Sci U S A 2007;104(29):12187–92. [PubMed: 17616583]

Boly M, Tshibanda L, Vanhaudenhuyse A, Noirhomme Q, Schnakers C, Ledoux D, Boveroux P, Garweg C, Lambermont B, Phillips C, Luxen A, Moonen G, Bassetti C, Maquet P, Laureys S. Functional connectivity in the default network during resting state is preserved in a vegetative but not in a brain dead patient. Human Brain Mapping 2009;30(8):2393–400. [PubMed: 19350563]

Cho S, Fujigaki T, Uchiyama Y, Fukusaki M, Shibata O, Sumikawa K. Effects of sevoflurane with and without nitrous oxide on human cerebral circulation. Transcranial Doppler study. Anesthesiology 1996;85(4):755–760. [PubMed: 8873545]

Crick F, Koch C. A framework for consciousness. Nat Neurosci 2003;6:119–126. [PubMed: 12555104]

Deshpande G, LaConte S, Peltier S, Hu X. Integrated local correlation: a new measure of local coherence in fMRI data. Human Brain Mapping 2009;30:13–23. [PubMed: 17979117]

Donoho, DL. Progress in wavelet analysis and WVD: a ten minute tour. In: Meyer, Y.; Roques, S., editors. Progress in wavelet analysis and applications. Frontières Ed; 1993. p. 109-128.

Donoho DL. De-noising by soft-thresholding. IEEE Trans. on Inf. Theory 1995;41(3):613–627.

Eichele T, Debener S, Calhoun VD, Specht K, Engel AK, Hugdahl K, von Cramon DY, Ullsperger M. Prediction of human errors by maladaptive changes in event-related brain networks. Proc Natl Acad Sci U S A 2008;105(16):6173–8. [PubMed: 18427123]

Evans, AC.; Collins, DL.; Mills, SR.; Brown, ED.; Kelly, RL.; Peters, TM. 3D statistical neuroanatomical models from 305 MRI volumes. Proceedings of the IEEE-Nuclear Science Symposium and Medical Imaging Conference; 1993. p. 1813-1817.

Franks NP. Molecular targets underlying general anaesthesia. British Journal of Pharmacology 2006;147 (Suppl 1):S72–81. [PubMed: 16402123]

Galinkin JL, Janiszewski D, Young CJ, Klafta JM, Klock PA, Coalson DW, Apfelbaum JL, Zacny JP. Subjective, psychomotor, cognitive, and analgesic effects of subanesthetic concentrations of sevoflurane and nitrous oxide. Anesthesiology 1997;87:1082–1088. [PubMed: 9366460]

Greicius MD, Krasnow B, Reiss AL, Menon V. Functional connectivity in the resting brain: a network analysis of the default mode hypothesis. Proc. Natl. Acad. Sci. U.S.A 2003;100(1):253–258. [PubMed: 12506194]

Greicius MD, Srivastava G, Reiss AL, Menon V. Default-mode activity distinguishes Alzheimer's disease from healthy aging: Evidence from functional MRI. Proc. Natl. Acad. Sci. U.S.A 2004;101(13): 4637–4642. [PubMed: 15070770]

Greicius MD, Kiviniemi V, Tervonen O, Vainionpää V, Alahuhta S, Reiss AL, Menon V. Persistent default-mode network connectivity during light sedation. Hum Brain Mapp 2008;29(7):839–47. [PubMed: 18219620]

Hayes, M. Statistical Digital Signal Processing and Modeling. John Wiley & Sons; 1996.

Heinke W, Schwarzbauer C. Subanesthetic isoflurane affects task-induced brain activation in a highly specific manner: a functional magnetic resonance imaging study. Anesthesiology 2001;94:973–981. [PubMed: 11465623]

Honey CJ, Sporns O, Cammoun L, Gigandet X, Thiran JP, Meuli R, Hagmann P. Predicting human resting-state functional connectivity from structural connectivity. Proc Natl Acad Sci U S A 2009;106:2035–40. [PubMed: 19188601]

Horovitz SG, Braun AR, Carr WS, Picchioni D, Balkin TJ, Fukunaga M, Duyn JH. Decoupling of the brain's default mode network during deep sleep. Proc Natl Acad Sci U S A 2009;106(27):11376–81. [PubMed: 19549821]

Horovitz SG, Fukunaga M, de Zwart JA, van Gelderen P, Fulton SC, Balkin TJ, Duyn JH. BOLD fMRI resting state activity and the network of default mode brain function. Proc. ISMRM 2006;14:531.

Ibrahim AE, Taraday JK, Kharasch ED. Bispectral index monitoring during sedation with sevoflurane, midazolam, and propofol. Anesthesiology 2001;95:1151–1159. [PubMed: 11684984]

Imas OA, Ropella KM, Ward BD, Wood JD, Hudetz AG. Volatile anesthetics disrupt frontal-posterior recurrent information transfer at gamma frequencies in rat. Neurosci Lett 2005;387(3):145–50. [PubMed: 16019145]

John ER, Prichep LS, Kox W, Valdés-Sosa P, Bosch-Bayard J, Aubert E, Tom M, di Michele F, Gugino LD. Invariant reversible QEEG effects of anesthetics. Conscious Cogn 2001;10(2):165–83. [PubMed: 11414713]

Kaisti KK, Långsjö JW, Aalto S, Oikonen V, Sipilä H, Teräs M, Hinkka S, Metsähonkala L, Scheinin H. Effects of sevoflurane, propofol, and adjunct nitrous oxide on regional cerebral blood flow, oxygen consumption, and blood volume in humans. Anesthesiology 2003;99(3):603–13. [PubMed: 12960544]

Kaisti KK, Metsähonkala L, Teräs M, Oikonen V, Aalto S, Jääskeläinen S, Hinkka S, Scheinin H. Effects of surgical levels of propofol and sevoflurane anesthesia on cerebral blood flow in healthy subjects studied with positron emission tomography. Anesthesiology 2002;96(6):1358–70. [PubMed: 12170048]

Kerssens C, Hamann S, Peltier S, Hu XP, Byas-Smith MG, Sebel PS. Attenuated brain response to auditory word stimulation with sevoflurane: a functional magnetic resonance imaging study in humans. Anesthesiology 2005;103(1):11–9. [PubMed: 15983451]

Kerssens C, Glielmi C, Peltier S, Sebel P, Hu X. Increased Resting-State Functional Connectivity during Light Sedation with Propofol. Anesthesiology 2008;109:A1306.

Kiviniemi VJ, Haanpaa H, Kantola JH, Jauhiainen J, Vainionpaa V, Alahuhta S, Tervonen O. Midazolam sedation increases fluctuation and synchrony of the resting brain BOLD signal. Magnetic Resonance Imaging 2005;23(4):531–537. [PubMed: 15919598]

Kolbitsch C, Lorenz IH, Hörmann C, Kremser C, Schocke M, Felber S, Moser PL, Hinteregger M, Pfeiffer KP, Benzer A. Sevoflurane and nitrous oxide increase regional cerebral blood flow (rCBF) and regional cerebral blood volume (rCBV) in a drug-specific manner in human volunteers. Magn Reson Imaging 2001;19(10):1253–60. [PubMed: 11804751]

Liu H, Liu Z, Liang M, Hao Y, Tan L, Kuang F, Yi Y, Xu L, Jiang T. Decreased regional homogeneity in schizophrenia: a resting state functional magnetic resonance imaging study. Neuroreport 2006;17 (1):19–22. [PubMed: 16361943]

Liu, Y.; Wang, K.; Yu, C.; He, Y.; Zhou, Y.; Liang, M.; Wang, L.; Jiang, T. Regional homogeneity. 2008.

Marcar VL, Schwarz U, Martin E, Loenneker T. How depth of anesthesia influences the blood oxygenation level-dependent signal from the visual cortex of children. American Journal of Neuroradiology 2006;27(4):799–805. [PubMed: 16611767]

Logothetis N, Pauls J, Augath M, Trinath T, Oeltermann A. Neurophysiological investigation of the basis of the fMRI signal. Nature 2001;412:150–157. [PubMed: 11449264]

Lorenz IH, Kolbitsch C, Hörmann C, Schocke M, Felber S, Zschiegner F, Hinteregger M, Kremser C, Pfeiffer KP, Benzer A. Subanesthetic concentration of sevoflurane increases regional cerebral blood flow more, but regional cerebral blood volume less, than subanesthetic concentration of isoflurane in human volunteers. Journal of Neurosurgical Anesthesiology 2001;13(4):288–295. [PubMed: 11733659]

Mashour GA. Consciousness unbound: toward a paradigm of general anesthesia. Anesthesiology 2004;100:428–433. [PubMed: 14739820]

Matta BF, Heath KJ, Tipping K, Summors AC. Direct cerebral vasodilatory effects of sevoflurane and isoflurane. Anesthesiology 1999;91(3):677–680. [PubMed: 10485778]

Nickalls RW, Mapleson WW. Age-related iso-MAC charts for isoflurane, sevoflurane and desflurane in man. British Journal of Anesthesia 2003;91(2):170–174.

Pagnoni, G.; Cekik, M.; Drake, DF.; Fornwalt, F.; Raison, CL.; Berns, GS. Topography and dynamics of resting state networks during meditation. Proceedings of the Annual Meeting of the Society for Neuroscience; Atlanta, GA. 2006. p. 364.122006

Pagnoni G, Guo Y. A unified framework for group independent component analysis for multi-subject fMRI data. NeuroImage. 2008 in press.

Pang GF, Wang SH, Ren YL, Ma L, Chen J, Xing W, Dong X. Cognitive development of normal school age children: a resting-state fMRI study. Zhonghua Yi Xue Za Zhi 2009;89(19):1313–7. Article in Chinese. [PubMed: 19615183]

Peltier SJ, Kerssens C, Hamann SB, Sebel PS, Byas-Smith M, Hu X. Functional connectivity changes with concentration of sevofurane anesthesia. NeuroReport 2005;16(3):285–288. [PubMed: 15706237]

Peltier SJ, Kerssens C, Hamann SB, Sebel PS, Byas-Smith M, Hu X. Default mode functional connectivity altered by sevoflurane anesthesia. Proc. ISMRM 2006;14:3260.

Raichle ME, MacLeod AM, Snyder AZ, Powers WJ, Gusnard DA, Shulman GL. A default mode of brain function. Proc. Natl. Acad. Sci. U.S.A 2001;98(2):676–682. [PubMed: 11209064]

Ramani R, Qiu M, Constable RT. Sevoflurane 0.25 MAC preferentially affects higher order association areas: a functional magnetic resonance imaging study in volunteers. Anesthesia and Analgesia 2007;105(3):648–655. [PubMed: 17717218]

Razavi M, Eaton B, Paradiso S, Mina M, Hudetz AG, Bolinger L. Source of low-frequency fluctuations in functional MRI signal. Journal of Magnetic Resonance Imaging 2008;27(4):891–897. [PubMed: 18383250]

Ries CR, Puil E. Mechanism of anesthesia revealed by shunting actions of isoflurane on thalamocortical neurons. J Neurophysiol 1999;81:1795–1801. [PubMed: 10200213]

Shi F, Liu Y, Jiang T, Zhou Y, Zhu W, Jiang J, Liu H, Liu Z. Regional homogeneity and anatomical parcellation for fMRI image classification: application to schizophrenia and normal controls. Med Image Comput Comput Assist Interv Int Conf Med Image Comput Comput Assist Interv 2007;10 (2):136–43.

Stefanovic B, Warnking JM, Rylander KM, Pike GB. The effect of global cerebral vasodilation on focal activation hemodynamics. NeuroImage 2006;30(3):726–34. [PubMed: 16337135]

Strang, G.; Ngugen, T. Wavelets and Filter Banks. Cambridge University Press; 1996.

Uddin LQ, Kelly AM, Biswal BB, Xavier Castellanos F, Milham MP. Functional connectivity of default mode network components: correlation, anticorrelation, and causality. Human Brain Mapping 2009;30:625–37. [PubMed: 18219617]

Veselis RA. Anesthesia - a descent or a jump into depths. Conscious Cogn 2001;10:230–235. [PubMed: 11414717]

Veselis RA, Feshchenko VA, Reinsel RA, Dnistrian AM, Beattie B, Akhurst TJ. Thiopental and propofol affect different regions of the brain at similar pharmacologic effects. Anesth Analg 2004;99:399–408. [PubMed: 15271714]

Veselis RA, Pryor KO, Reinsel RA, Mehta M, Pan H, Johnson RJ. Low-dose propofol-induced amnesia is not due to a failure of encoding: left inferior prefrontal cortex is still active. Anesthesiology 2008;109(2):213–24. [PubMed: 18648230]

Veselis RA, Reinsel RA, Feshchenko VA, Dnistrian AM. A neuroanatomical construct for the amnesic effects of propofol. Anesthesiology 2002;97:329–337. [PubMed: 12151921]

Wei W. The effects of systematic sampling and temporal aggregation on causality - A cautionary note. Journal of the American Statistical Association 1982;77(378):316320.

White NS, Alkire MT. Impaired thalamocortical connectivity in humans during general-anesthetic-induced unconsciousness. NeuroImage 2003;19:402–411. [PubMed: 12814589]

Wig GS, Grafton ST, Demos KE, Wolford GL, Petersen SE, Kelley WM. Medial temporal lobe BOLD activity at rest predicts individual differences in memory ability in healthy young adults. Proc Natl Acad Sci U S A 2008;105(47):18555–60. [PubMed: 19001272]

Wilcoxon F. Individual Comparisons by Ranking Methods. Biometrics 1945;1:80–83.

Wu T, Long X, Zang Y, Wang L, Hallett M, Li K, Chan P. Regional homogeneity changes in patients with Parkinson's disease. Human Brain Mapping 2009;30(5):1502–10. [PubMed: 18649351]

Yao Z, Wang L, Lu Q, Liu H, Teng G. Regional homogeneity in depression and its relationship with separate depressive symptom clusters: a resting-state fMRI study. Journal of Affective Disorders 2009;115(3):430–8. [PubMed: 19007997]

Yuan Y, Zhang Z, Bai F, Yu H, Shi Y, Qian Y, Liu W, You J, Zhang X, Liu Z. Abnormal neural activity in the patients with remitted geriatric depression: a resting-state functional magnetic resonance imaging study. Journal of Affective Disorders 2008;111(2–3):145–52. [PubMed: 18372048]

Zang Y, Jiang T, Lu Y, He Y, Tian L. Regional homogeneity approach to fMRI data analysis. Neuroimage 2004;22:394–400. [PubMed: 15110032]

Zhu CZ, Zang YF, Cao QJ, Yan CG, He Y, Jiang TZ, Sui MQ, Wang YF. Fisher discriminative analysis of resting-state brain function for attention-deficit/hyperactivity disorder. NeuroImage 2008;40(1): 110–20. [PubMed: 18191584]

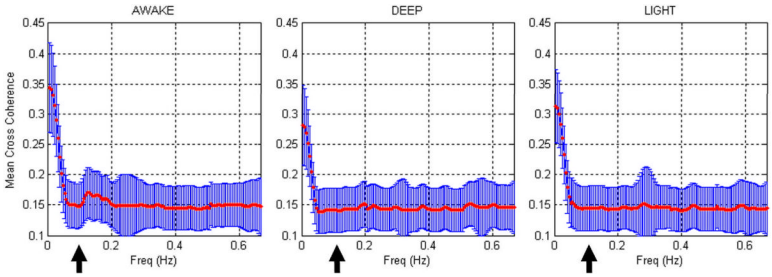

Figure 1.

The cross coherence function obtained from all the subjects in the awake (left), deep (middle) and light (right) states. The mean curve is shown in red and standard deviation as blue bars. The cross coherence function provides a frequency-specific decomposition of ILC. The high frequency coherence components (>0.1 Hz), which typically contain the effects of physiological artifacts, were significantly lesser in magnitude and remained relatively constant between the three states in comparison to the low frequency coherence components (<0.1 Hz) which are thought to be physiologically relevant. The arrow in the figure shows the cut off frequency of 0.1 Hz. Therefore, it can be inferred that the ILC differences between the three states were mainly driven by the differences in the low frequency coherence components

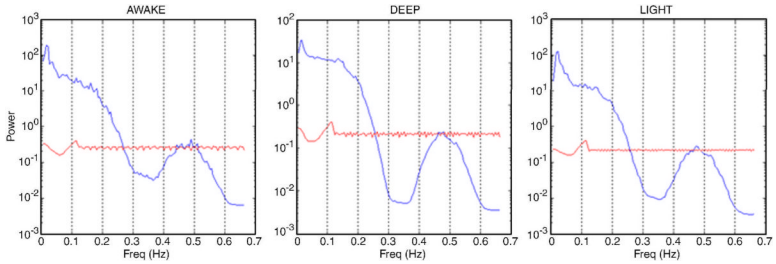

Figure 2.

The mean power spectra of the fMRI time series inside the brain (blue) and the downsampled physiological time series (red) for the awake (left), deep (middle) and light (right) states. Note that the power on the y-axis is represented on a logarithmic scale and is different for the deep state in order to highlight the fact that downsampled physiological time series had a power less than one compared to a power of 10–100 for fMRI time series inside the brain. Therefore, it can be inferred that downsampling did not alias the physiological rhythms into the low frequency band (<0.1 Hz)

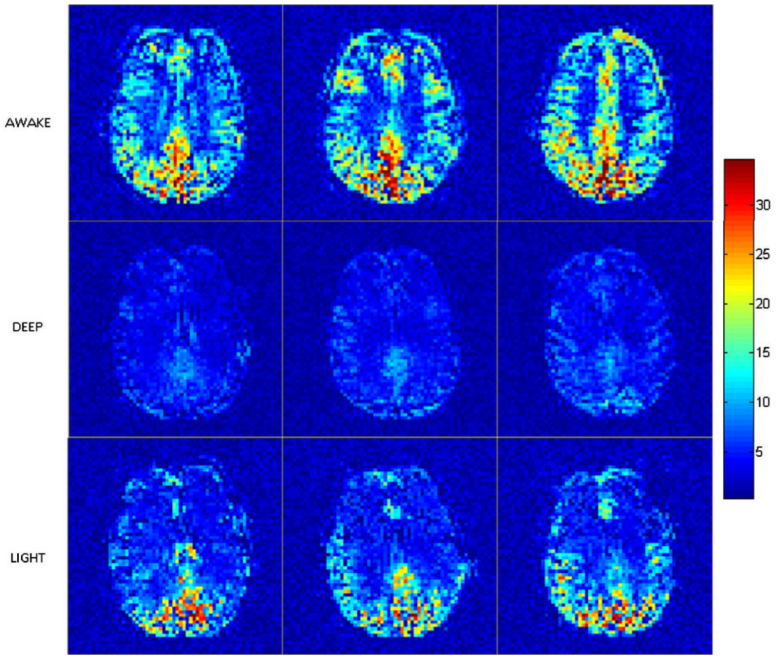

Figure 3.
Group ILC maps for the awake (top), deep (middle) and light (bottom) anesthetic states in EPI space. Slices containing the default mode network are displayed. ILC was greater in areas of high metabolism such as posterior cingulate in the awake state. Global reduction of ILC was observed in the deep state. ILC recovered in the posterior areas in the light state, but remained attenuated in the frontal areas

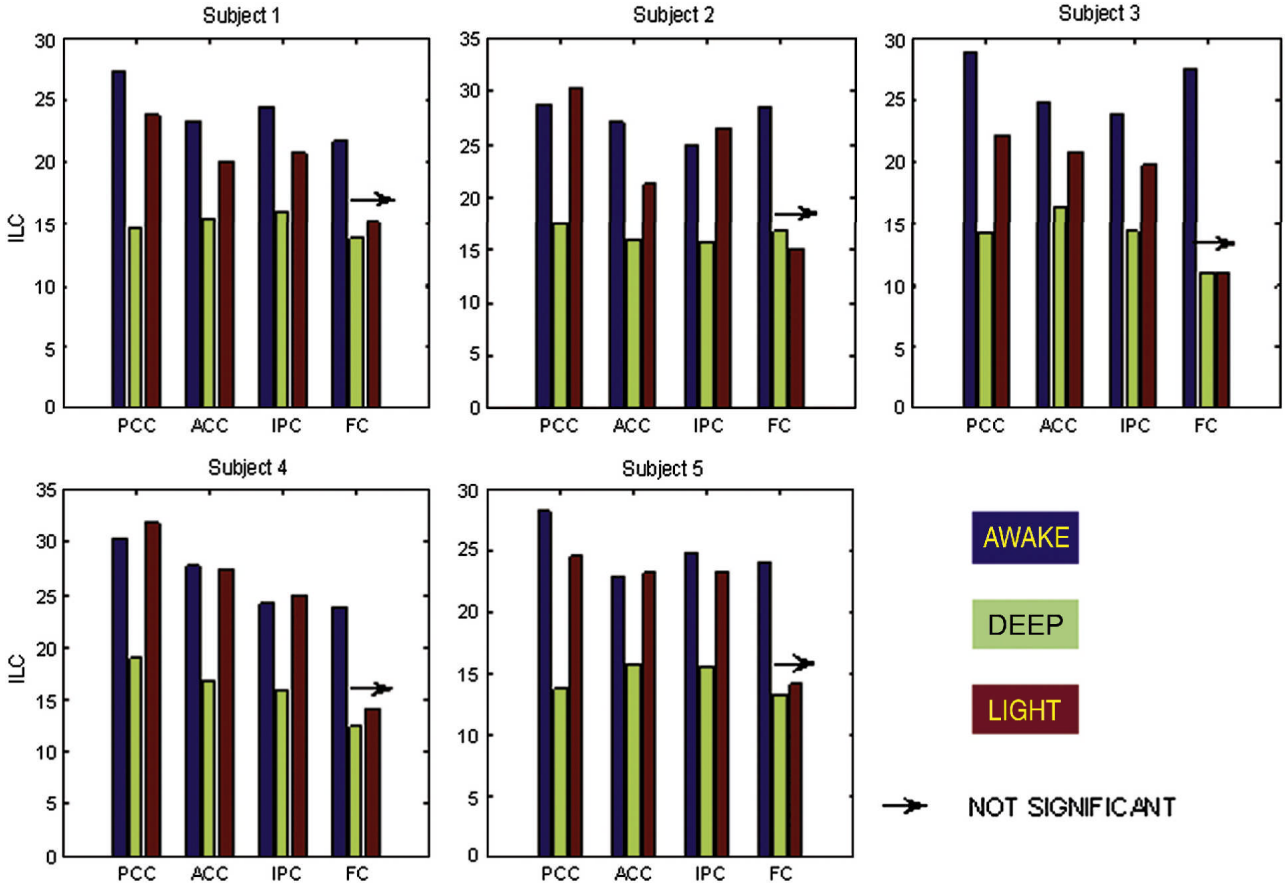

Figure 4.

ROI-specific ILC values for all the five subjects. The awake and deep states were statistically different ($p<0.05$) for each ROI in every subject while the deep and light states were statistically different ($p<0.05$) for PCC, ACC and IPC in all the subjects. The arrow indicates that the ILC transition from deep to light state was not significant ($p>0.05$) for FC in all subjects. PCC: Posterior cingulate cortex, ACC: Anterior cingulate cortex, IPC: Inferior parietal cortex, FC: Frontal cortex. The color of the bar indicates the anesthetic state. Blue: awake, Green: deep and Red: light

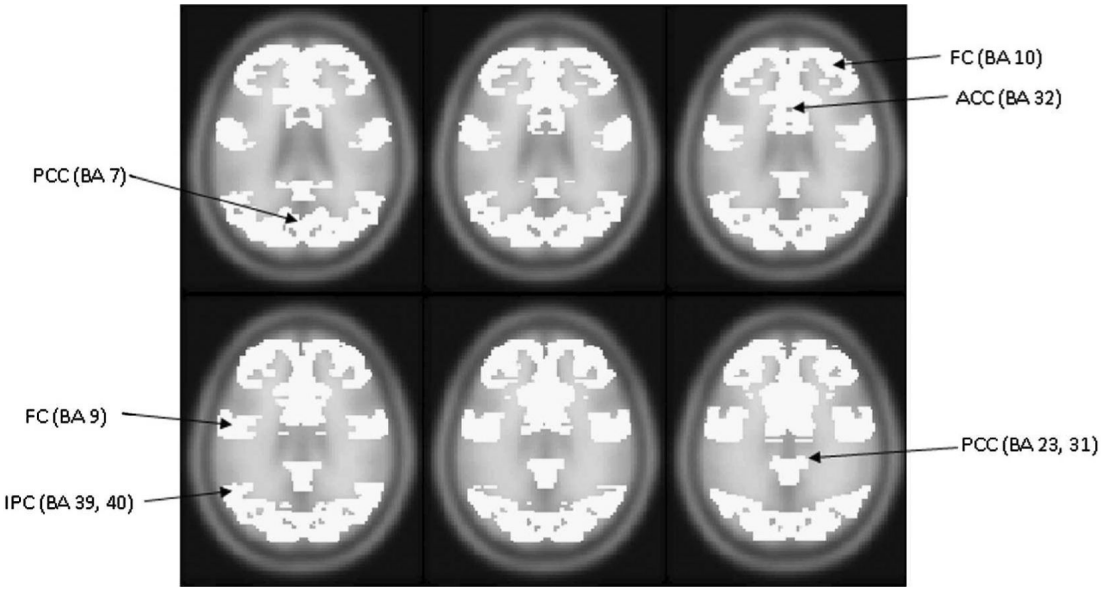

Figure 5.
The resting-state default mode mask in MNI space. Abbreviations – PCC: posterior cingulate cortex, ACC: anterior cingulate cortex, IPC: inferior parietal cortex, FC: frontal cortex, BA: Brodmann area